Title

Quantitative Assessment of Alkali-Activated Materials: Environmental Impact and Property Assessments

Journal

Journal of Infrastructure Systems, 26(3)

ISSN

1076-0342

Authors

Cunningham, Patrick R

Miller, Sabbie A

Publication Date

2020-09-01

DOI

10.1061/(asce)is.1943-555x.0000556

Quantitative assessment of alkali-activated materials: environmental impact and property assessments

Patrick R. Cunningham [a], Sabbie A. Miller, Ph.D. [b, †]
[a] Department of Civil and Environmental Engineering, University of California, Davis
2001 Ghausi Hall, One Shields Ave, Davis, CA, 95616
[b] Department of Civil and Environmental Engineering, University of California, Davis
2001 Ghausi Hall, One Shields Ave, Davis, CA, 95616
[†] Corresponding Author: T +1 530 754 6407, E sabmil@ucdavis.edu

Abstract:
This study compares greenhouse gas (GHG) emissions, embodied energy, and air pollutant emissions of alkali-activated mortars and conventional portland cement-based mortars. Alkali-activated materials (AAMs) do not require the use of portland cement to offer cementitious properties; these materials can valorize industrial waste streams and non-cementitious natural resources. In this work, several AAMs containing blast furnace slag and natural pozzolans were examined. Comparisons were drawn both based on the production on 1 m^3 of material and based on ratios of GHG emissions to mortar strength. To facilitate robust assessments, mechanical and material properties were determined. GHG emissions, embodied energy, as well as NO_X, SO_X, CO and Pb emissions for the alkali-activated mortars were lower than their conventional counterparts. However, the AAMs exhibited higher VOC and PM_{10} emissions. When ratios of GHG emissions to strength were examined, results indicated that the lower environmental impacts of AAMs could be desirable relative to portland cement mortars, even when the AAMs displayed lower mechanical strength. These findings suggest, depending on application, AAMs could contribute to environmental impact mitigation strategies.

Keywords:
Alkali-activated materials (AAMs); Natural pozzolans (NP); Blast-furnace slag (BFS); Environmental impact assessment; Greenhouse gas (GHG) emissions; Air pollutant emissions

Declarations of interest: none

Introduction

The demand for hydraulic cement and cement-based materials has escalated sharply within the past several years and with this increase in demand, there has been a rise in environmental impacts from their production. Between 1926 and 2000, the cumulative world production of hydraulic cement was 40.5 billion metric tons; between 2001 and 2015, there was a cumulative 44.5 billion metric tons of hydraulic cement production, nearly 1.1 times the amount made in the preceding 75 years (Kelly and van Oss 2014; van Oss 2017). The high production of hydraulic cement occurring now, approximately 4 billion metric tons annually (van Oss 2017), is causing notable environmental impacts globally: a reported 8-9% of anthropogenic greenhouse gas (GHG) emissions, 2-3% of energy demand, and 9% of industrial water withdrawals are attributed to the production of cement-based materials every year (Miller *et al.,* 2016a; Monteiro *et al.,* 2017; Miller *et al.,* 2018a). This consumption requires high inputs of natural resources and the associated environmental impacts from cement and cement-based materials production have sparked many efforts to use alternative materials with potentially lower burdens on the environment. These efforts include more efficient use of natural pozzolans and other mineral admixtures (Sánchez Berriel *et al.,* 2016), use of agricultural wastes as mineral admixtures (Gursel *et al.,* 2016; Miller *et al.,* 2019), the development of alternative cements such as those made based on alternative clinkers (Gartner and Sui 2018), and alkali-activated materials (AAMs) (Provis 2018).

In this work, the properties of AAMs are explored to better understand the confluence of their material properties and their environmental impacts from production. AAMs have been researched for decades as alternative materials for conventional hydraulic cements and are now of key interest as a means to reduce environmental burdens associated with cement-based materials (Provis 2018). The use of alkali-activation to create binders with similar properties to

cement was first introduced in 1940 using blast-furnace slag (Juenger *et al.,* 2011); earlier limitations in the popularity of studying these materials has been overcome by their potential environmental benefits. AAM mixture design methodology and construction techniques are similar to traditional concretes, easing implementation in practice (Provis 2018). AAMs have been used in specialized applications in Asia, America, and Europe (Juenger *et al.,* 2011).

Unlike traditional hydraulic cements that react with water, alkali-activated materials can be made through use of a variety of alkali-activators and solid precursors. Most commonly, the solid precursors used in the production of these alkali-activated materials are industrial by-products, such as fly ash and ground granulated blast-furnace slag, and natural compounds, such as natural pozzolans and calcined clays (Provis 2018; Robayo-Salazar *et al.,* 2018). Often, the alkali-activators used are sodium or potassium hydroxides or silicates (Provis 2018). Due to the range in chemical and mineralogical compositions that can be used in the formation of AAMs, a range of hardened properties can be achieved (Habert *et al.,* 2011; Heath *et al.,* 2014). Promising work is being conducted to better understand how the selection of solid precursors and alkali-activators as well as their proportions can be utilized to influence the AAM properties (e.g., (Abdalqader *et al.,* 2016)). Yet the development of standards to achieve desired properties has proven challenging and is an area requiring more research (Provis 2018; Robayo-Salazar *et al.,* 2018).

While AAMs have been discussed as a potential means to reduce environmental impacts of the cement-based materials industry, environmental impact assessments for the production of these AAMs remain limited. Most of the literature on assessing environmental impacts of AAMs focuses on greenhouse gas emissions from their production, often drawing comparisons to portland cement (PC) and PC-based materials. For example, Teh *et al.* (Teh *et al.,* 2017)

conducted hybrid life-cycle assessment (LCA) to assess embodied carbon of AAMs; Robayo-Salazar *et al.* (Robayo-Salazar *et al.,* 2018) studied global warming potential and global temperature change in CO_2-eq of natural pozzolan/ground granulated blast-furnace slag AAMs; Heath *et al.* (Heath *et al.,* 2014) examined global warming potential for clay-based AAMs; Yang *et al.* (Yang *et al.,* 2013) studied the carbon dioxide footprint for several AAMs; Turner and Collins (Turner and Collins 2013) assessed CO_2-eq emissions from AAMs. Because there are increasingly limited supplies of industrial by-products such as fly ash and granulated blast-furnace slag, some assessments have been conducted on the environmental impacts of AAMs relying more heavily on the use of natural resources, such as natural pozzolans and calcined clays (Heath *et al.,* 2014; Robayo-Salazar *et al.,* 2018); however, these studies also focused solely on impacts from the greenhouse gas emissions associated with production. Other studies have extended beyond greenhouse gas emissions to examine impacts such as cost and/or embodied energy: McLellan *et al.* (McLellan *et al.,* 2011) examined cost, greenhouse gas emissions, and energy; Ohno and Li (Ohno and Li 2018) examined greenhouse gas emissions and embodied energy. Few studies have examined multiple environmental impact categories in the assessment of AAMs: Habert *et al.* (Habert *et al.,* 2011) as well as Habert and Ouellet-Plamondon (Habert and Ouellet-Plamondon 2016) assessed 10 environmental impact categories using the CML weighting method; Yang *et al.* (Yang *et al.,* 2014) assessed 6 environmental impact categories: abiotic depletion, global warming potential, acidification potential, eutrophication potential, photochemical oxidation potential, and human toxicity potential; Jiang *et al.* (Jiang *et al.,* 2014) assessed global warming potentials, water use, cumulative energy demand, and potential environmental toxicity using the US Environmental Protection Agency's TRACI scheme. However, none of these studies concurrently considered environmental impacts

and mechanical properties and often materials assessed contained theoretical constituents as opposed to drawing comparisons with experimental results.

With this emphasis on the need to find alternative constituents for conventional cement-based materials in order to mitigate environmental impacts, understanding the material properties achieved in cementitious alternatives and the effects of their use on multiple environmental impact categories is critical. The objectives of this work were to perform combined mechanical property assessments and environmental impact assessments to determine the conditions under which AAMs can be used to mitigate environmental impacts from the cement-based materials industry. To perform this assessment, four AAM mortars were compared to three mortars made with a typical hydraulic PC as the primary binder. The AAM mixtures selected for analysis contained varying types of alkali-activators, at relatively low concentrations, and intentionally do not include Na_2SiO_3, which is currently cost-prohibitive to large-scale implementation. The environmental impacts examined include GHG emissions, embodied energy, and, to explore potential co-benefits or unintended consequences in use of AAMs, air pollutant emissions from the production of these different materials. Comparisons were drawn using both mechanical properties and environmental impacts to elucidate desirable attributes in AAMs. By elucidating material properties, commonly explored environmental impacts like GHG emissions, and less well characterized emissions like air pollutants, this work advances our understanding of engineering AAMs to be environmentally sustainable cementitious material alternatives.

Methods

Environmental Impact Assessment

Scope of Assessment

Environmental impacts from the production of the AAMs analyzed in this work and the mortar made with PC were quantified for cradle-to-gate production (i.e., from raw material or by-product material acquisition through batching of the mortar). Figure 1 presents a diagram of the scope of analysis including constituents and manufacturing stages considered in this work. At each of these stages, thermal energy, electricity, transportation, and raw-material derived emissions were assessed. Three functional units of assessment were used in this work. Initial impact assessments were determined using a cubic meter of mortar with production taking place in Sacramento, California. Two sets of emissions and embodied energy were quantified as part of this assessment. The first set of emissions was greenhouse gas (GHG) emissions, namely carbon dioxide (CO_2), methane (CH_4), and nitrous oxide (N_2O). These emissions are presented as a cumulative value in CO_2-eq emissions based on the Intergovernmental Panel on Climate Change (IPCC) 100 year time horizon global warming potentials (Solomon *et al.,* 2007). The second set of emissions considered was criteria air pollutants and precursors to criteria air pollutants: namely nitrogen oxides (NO_X), sulfur oxides (SO_X), volatile organic compounds (VOC), carbon monoxide (CO), particulate matter 10 microns or smaller (PM_{10}), and lead (Pb). These emissions were selected for study due to prevalent interest in means to reduce GHG emissions from cementitious material production (e.g., (Scrivener *et al.,* 2017)) and concern regarding air pollutant emissions from the cement manufacturing stages (Chatterjee 2011). Finally, embodied energy associated with each material and process was assessed. The GHG emissions, CO_2, CH_4, and N_2O, were presented cumulatively as is common practice in assessment of cementitious

materials; however, because the effects of air pollutant emissions vary depending on several factors, such as local air conditions and human intake fraction, the air pollutant emissions were not weighted into a single score.

While environmental impacts from the construction, use, and end of life of the mixtures were considered outside the scope of this research, two additional functional units that incorporate inputs used in concrete design were assessed. For these cases, a modified functional unit that presents cradle-to-gate GHG emissions to compressive strength as a ratio and GHG emissions to tensile strength as a ratio were examined. These comparisons were drawn utilizing experimental data discussed in the subsequent sections. Such ratios or similar ones have been presented in concrete literature to better represent the influence of cement-based material behavior considering material properties and their influence on parameters such as volume of material needed for required performance (Damineli *et al.*, 2010; Gursel *et al.*, 2016; Miller *et al.*, 2016b). Specifically, for the incorporation of tensile or compressive strength, such ratios of comparison would be useful in applications where these strengths were the primary determining factor in the volume of cement-based material required; for example, design for use in an axially loaded member of fixed length that is not susceptible to buckling.

Environmental Impact Modeling

To quantify environmental impacts from the production of AAMs and draw comparisons with mechanical properties, both environmental impact and experimental assessments were performed for a small subset of potential AAMs, namely, the seven mortar mixtures specified in Table 1. A cradle-to-gate analysis of energy requirements as well as sources of emissions for each constituent and process necessary to produce the mortars was performed. Inputs and

assumptions used to assess these environmental impacts from the production of each of the mortar constituents.

The PC was modeled as being comprised of approximately 95% clinker and 5% gypsum by mass with a 65% lime-based clinker. The PC was modeled as produced locally and transported a distance of 50 km by truck. The kiln efficiency was modeled based on an average of the types of kilns used in California, which have been reported to be ~15% dry kilns and ~85% precalciner kilns (Marceau *et al.*, 2006). The kiln fuel mix was modeled based on the United States average kiln fuel mix as reported by the United States Geological Survey (van Oss 2015). GHG and air pollutant emissions as well as the embodied energy from these fuels and the required energy input for manufacturing and transportation as well as raw-material derived emissions were based on the University of California, Berkeley GreenConcrete tool (Gursel and Horvath 2012). The electricity required in the cement production process was based on the efficiency of fuel conversion and electricity demand for each phase of production, outlined in Table 2. The electricity grid for production was modeled as the average California electricity grid from 2016 (CEC 2018) with emissions for each electricity source modeled based on conversion efficiency and combustion products.

Ground granulated blast furnace slag (GBS) is not a material produced in California. As such, it was modeled as being produced in and imported from Pennsylvania, a large producer of steel and the industrial by-product of GBS (Platts 2014). The transportation for this GBS was modeled as 4500 km by rail. The electricity required for collection and processing GBS was based on the GreenConcrete tool (Gursel and Horvath 2012). This electricity requirement was modeled as being met through use of the average Pennsylvania electricity grid from 2014 (USDOE 2015). Impacts for this material considered collection, any refinement necessary, and

transportation; no allocation methods that would attribute any impacts from the production of iron were incorporated in this assessment.

While GBS is not produced in California, there are NP deposits available near the production location of Sacramento, California. The NP was modeled as being acquired in and transported from Northwestern Nevada, specifically a distance of 300 km by rail to Sacramento. Electricity required for material acquisition and environmental impacts were based on the GreenConcrete tool (Gursel and Horvath 2012) and the electricity grid was taken as the Nevada average grid in 2014 (USDOE 2016).

The alkali-activators used for the AAMs produced for this work included sodium hydroxide (NaOH), sodium carbonate (Na_2CO_3), and sodium sulfate (Na_2SO_4). Each of these chemicals was modeled as being transported 1000 km by truck to the batching site. Transportation emissions were estimated using the same model present in the GreenConcrete tool (Gursel and Horvath 2012) to maintain consistency with other constituent transportation models. GHG and air pollutant emissions as well as embodied energy for the production of these chemicals were based on United States production values. For Na_2CO_3 and Na_2SO_4, impacts were modeled based on inventory data from (LTS 2016), and for NaOH, these impacts were modeled based on data from (NREL 2012).

The fine aggregates were modeled as locally sourced. This modeling included transportation of aggregates over a distance of 50 km by truck from the quarry to the batching site. Energy required for material acquisition and processing (e.g., sieving) was based on the GreenConcrete tool (Gursel and Horvath 2012) in which emissions were assessed based on both energy, using the California grid (CEC 2018), as well as raw-material derived particulate matter emissions.

The acquisition, processing, and transportation for each of the constituents were considered, as was each of the processes necessary for the production of the mortars. Batching and curing was modeled as occurring in Sacramento, California. While all specimens were considered to require batching, only the mixtures cured at an elevated temperature for the first three days of curing were considered to require additional energy input to reach that elevated temperature. Batching energy required was based on the GreenConcrete tool (Gursel and Horvath 2012), using the California electricity grid (CEC 2018), and was assumed to occur at a central mixing plant. The curing energy required for the elevated temperature curing and associated fuel mix were based on Marceau *et al.* (Marceau *et al.,* 2007), with emissions for each fuel source based on a median of data reported by (USEPA 1995a, 2001; Gomez *et al.,* 2007; GREET 2010). While the AAMs did not contain any cement, they were modeled as using the same batching energy and emissions models as the control mortars. This assumption was made because the primary difference in batching was the use of an alkaline solution for the AAM mortars instead of solely distilled water, as was used for the PC mortars; as such, the batching impacts would be approximately equivalent.

Materials

In California, there is limited combustion of coal for electricity, thus limiting availability of fly ash. To assess the potential for using other pozzolanic materials in the place of fly ash, this work examined the use of locally sourced Class N Natural Pozzolans (NP). These natural pozzolans were combined with ground granulated blast-furnace slag (GBS) to act as a solid precursor in the alkali activated materials studied.

Ordinary Portland Cement and Supplementary Cementitious Materials

The powder materials used in the mixtures are ASTM Type II/V PC, GBS, and NP. The PC and GBS were obtained from the Lehigh Southwest Cement Co in Stockton, CA. ASTM Type II/V PC was selected because given the characteristics of California soils, sulfate-induced deterioration of concrete is a prevalent concern. Typically, Type II/V cements are used to improve the durability of the cement-based materials manufactured in the State. The NP was obtained from the Nevada Cement Company in Fernley, Nevada. The GBS was compliant with ASTM C 989-14 Grades 100 and 120; the NP was compliant with ASTM 618-17a and AASHTO M 295 specifications for a class "N" pozzolan.

Alkali Activators

For the alkali sources, solutions were obtained and mixed with distilled water to achieve the desired weight ratio stipulated in Table 1. The sodium sulfate (Na_2SO_4 22.2% w/v solution) was obtained from the Ricca Chemical Company. The sodium carbonate (Na_2CO_3 1N aqueous solution) was obtained from VWR BDH chemicals. The sodium hydroxide (NaOH 50% w/w solution) were obtained from Sigma Aldrich. The AAM mortars were prepared using these solutions and contained no PC.

Aggregates

The mortar batched for this work used natural sand as the fine aggregate (with a 99.8% passing rate through a #4 sieve). This natural sand was locally sourced from Cashe Creek, CA.

Mixtures

The mortar mixture proportions used are shown in Table 1. The GBS and NP were used in equal proportions to act as the solid precursor in the AAM mixtures; the type and quantity of alkali-activators was varied. For this work, the AAM mixtures were compared to 3 control

mixtures produced with PC: one containing no mineral admixtures, one containing GBS as a partial replacement for PC, and one containing NP as a partial replacement for PC. A 33% replacement level for the PC-based mixtures was selected based on the prevalence of this, or nearly this, replacement ratio in the literature as a common level for both types of mineral admixtures (e.g., (Oner and Akyuz 2007; Meddah 2015)). The water to powder ratio was fixed at 0.5 for all mixtures. Alkali-activator types and quantities were based on a survey of the literature, namely (Bakharev 2005; Rattanasak and Chindaprasirt 2009; Ryu *et al.*, 2013; Abdalqader *et al.*, 2016; Zhuang *et al.*, 2016; Robayo-Salazar *et al.*, 2018), and were selected to represent different activators. Mixtures not containing sodium silicate were intentionally selected due to high commercial costs of the solution at the moment, potentially limiting its use in certain applications. Aggregate mass was varied slightly to account for differences in the density of the powders used.

Experimental Characterization

Specimen Preparation

To perform experimental characterization of specimens, mortar was batched using a Hobart A200 dough mixer. Fine aggregates were oven dried at 100°C to remove excess moisture. The dry constituents, that is, the powder and the aggregates were mixed for 1 minute in the dough mixer prior to the addition of the aqueous solutions. The aqueous solutions, namely, distilled water for mixtures 1, 2, and 3, and the distilled water mixed with alkalis producing alkali solutions for the remaining mixtures, were then poured in and mixing recommenced for an additional 2 minutes. Batches were allowed to sit for 1 minute followed by a final mixing of 2 minutes. Batches were poured into their respective molds and vibrated for 30 seconds to remove entrapped air. Two sets of specimen sizes were made: 50.8mm × 101.6mm (2 inch × 4 inch)

cylinders and 76.2mm × 152.4mm (3 inch × 6 inch) cylinders. The smaller cylinders were used to determine compressive strength as well as splitting tensile strength; three specimens were assessed for each experiment. The larger cylinders were used to assess bulk density, void volume, and porosity. To assess the influence of specimen curing conditions, specimens from each batch were cured in one of two conditions: (i) Condition 1 - 100% RH, 25°C prior to testing; (ii) Condition 2 - 100% RH, 35°C for an initial curing period of 3 days, followed by 25°C at 100% RH prior to testing.

Compressive Strength of Mortar

The compressive strengths of the mortars were tested after 7, 14, and 28 days of curing. These curing periods were selected to determine early-age strength development. Experiments were conducted using a SoilTest CT-950 load frame and were based on adaptations of the protocol outlined in ASTM C39 (ASTM 2017a). Specimens were capped with sulfur mortar on one side and a rubber pad on the other. Testing was performed under deflection-control and continued until softening or failure occurred; maximum load was used to assess strength. Analysis of variance (ANOVA) was performed to determine statistical significance of difference in mechanical strength as a function of curing condition.

Tensile Strength of Mortar

The tensile strengths of the mortars were tested after 28 days of curing. Tensile strength was determined by splitting tensile testing based on adaptations of the protocol outlined in ASTM C496 (ASTM 2017b). Similar to compressive strength assessment, testing was performed in a SoilTest CT-950 load frame. Tensile strength was calculated based on the maximum load the materials could withstand.

Determination of Density and Absorption

Water absorption, void volume, and bulk density were determined for the mortars. Tests were performed on specimens cured for 28 days and were based on ASTM C642 (ASTM 2013). For testing, a submersion apparatus with a Mark 10 M3-100 Series 3 force gauge was used. Specimens were dried at 100-110°C in an oven and weighed every 24 hours until less than 0.5% weight fluctuation between two successive measurements to obtain a dry weight. Then, saturated surface-dry weight was obtained by submerging specimens in water and weighed every 24 hours until weight fluctuated less than 0.5% between two successive measurements. Specimens were placed in boiling water for 5 hours and allowed to cool for a minimum of 14 hours to determine a soaked, boiled, and surface-dry weight. Finally, specimens were suspended in water to determine apparent weight. These weights were used to inform water absorption, void volume, and bulk density for the mortars.

Results

Environmental Impact Results

Because the use of alkali-activated materials is often presented in the context of producing more sustainable alternatives to conventional PC concrete and mortar (e.g., (McLellan *et al.*, 2011; Heath *et al.*, 2014; Miller *et al.*, 2018b; Provis 2018; Robayo-Salazar *et al.*, 2018)), this work emphasized a robust quantification of environmental impacts from the production of AAM mortar. The most prevalent environmental impact for AAMs presented in the literature is their ability to offer lower GHG emissions relative to PC concrete. This ability is based on the lack of need for PC in AAMs and the knowledge the PC is the primary contributor to GHG emissions from concrete production (Miller *et al.*, 2016a). As can be seen from the GHG emissions assessment conducted for this work (Figure 2), the AAM mixtures assessed in this research did

contribute to lower GHG emissions than the PC mixtures, which were dominated by the emissions from cement production. For the PC mixtures, even with up to one third of the binder composed of a mineral admixture (i.e., NP or GBS), 85-99% of GHG emissions came from the production of the cement. This high level of GHG emissions was a function of the raw-material derived CO_2 emissions from the calcining process and the energy-derived GHG emissions from fuel combustion to kiln the raw materials at the requisite temperature for cement production. Despite the AAMs not containing PC, the GHG emissions to produce the AAM mixtures assessed in this work ranged from producing 15-40% of the GHG emissions as the conventional mortar counter parts. These relatively high GHG emissions for AAMs were reflective of a few factors: (a) while no allocation process was used to assign some of the environmental impacts from the production of pig iron to the GBS, the impacts associated with transporting it across the United States from Pennsylvania to California resulted in GHG emissions; (b) the production and transportation of the alkali-activators could lead to notable GHG emissions and they too were transported a relatively long distance by means of a high emitting vehicle, diesel trucks. For the AAM mortar mixtures assessed herein, the GBS contributed 40-70% of the total GHG emissions and the alkali-activators contributed 15-50% of the total GHG emissions, including transportation of materials to the batching site. While curing of the composites at an elevated temperature did lead to an increase in GHG emissions associated with the energy-demand, the contribution to GHG emissions remained lower than the material constituents, namely 3-18% of the total GHG emissions for the materials cured at 35°C.

While not as frequently discussed in the literature as GHG emissions, the production of PC and concrete leads to the production of air pollutant emissions (USEPA 1995b; Celik *et al.*, 2015; Gursel *et al.*, 2016). Due to the implications of air pollutant production on human health,

assessment of such pollutant emissions could be critical in policy development to guide the production of cementitious materials. For the mortar mixtures examined in this research, six air pollutant emissions were assessed and results for these assessments are presented in Figure 3. These results indicated that, similar to GHG emissions, the production of AAMs could lead to reductions in NO_X, SO_X, CO, and Pb emissions. For NO_X emissions, the AAMs led to a wide range in emissions reductions, namely 0-40% lower emissions than the PC-based mixtures. This wide range was a function of the variation in emissions noted for the PC mortars, which displayed higher NO_X emissions for Mixtures 1 and 2, but lower emissions for Mixture 3, a function of the NP requiring less transportation than the GBS. The AAMs could result in 30-40% lower NO_X emissions than the PC mortar and the PC/GBS mortar; however, the highest emitting AAM, Mixture 6, had very similar NO_X emissions to Mixture 3, the PC/NP mortar. For SO_X emissions, the AAMs offered 60-80% lower emissions than the PC-based mixtures. For CO and Pb emissions, the AAMs resulted in nearly 100% lower emissions than their conventional counterparts. In each of these cases, the AAMs were able to offer lower emissions because of the high contributions of NO_X, SO_X, CO, and Pb emissions from the production of PC. For PM_{10} emissions, the AAMs produced approximately 20-170% higher emissions than the conventional PC-based mixtures; however, a substantial contributor to particulate emissions both for Mixture 2 of the conventional mixtures and for the AAMs was the particulate emissions from the GBS. High particulate emissions were associated with the GBS from both the collection method modeled using the GreenConcrete tool (Gursel and Horvath 2012) and the long transportation distance. The contributions from transportation were again reflected in the PM_{10} emissions for the alkali-activators. Similar to the PM_{10} emissions, the production of VOCs was higher for the production of AAMs than for the PC-based mortars. These high VOC emissions were a function

of the production of the different alkali-activators, with the majority of their contribution to emissions coming from chemical production, followed by transportation by truck of alkali-activators to the batching site. While sodium sulfate offered lower VOC emissions per kg of production than sodium carbonate or sodium hydroxide, the emissions for each of these materials was notable when compared to the production of aggregates and the mineral admixtures assessed; the low emissions from the production of sodium carbonate did result in Mixture 5 having similar VOC emissions to several of the PC mortars. The transportation emissions associated with importing GBS from Pennsylvania resulted in the second highest contribution to total VOCs, but for the AAMs, the alkali-activators resulted in 95-99% of the VOC emissions from mortar production. These high VOC emissions led to the AAMs having 0.75 to 17 times the VOC emissions of the PC-based mixtures.

This work also assessed the embodied energy for the production of AAM mortars and compared results to those for PC-based mortars (see Figure 4). Results of the embodied energy assessment showed a high variability in impacts for the AAM materials. The highest embodied energy for the AAM mortars was for Mixture 6 cured at 35°C (i.e., condition 2) and the lowest was for Mixture 5 cured only at 25°C; there was a 3-fold difference between the embodied energies for these two mixtures. As would be expected, the PC, which required a large amount of energy in the pyroprocessing of clinker for cement, was the largest contributor to embodied energy for Mixtures 1-3. This high contribution to embodied energy for the PC-based mixtures resulted in the AAMs offering 10-80% lower embodied energy.

Experimental Results

Compressive Strength of Mortar

Early age compressive strength of the mortars cured in condition 1, consistently at 25°C, and condition 2, cured at 35°C for 3 days then cured at 25°C for the remainder, are shown in Figure 5. All mortars tested displayed an increase in compressive strength with time. The greatest increase in strength was exhibited by the mixture with PC and GBS cured consistently in 25°C (i.e., Mixture 2 in condition 1). This mixture showed an 11 MPa increase in strength between the 7-day strength and the 28-day strength, a 50% increase. Mixture 3, the mixture containing partial replacement of PC with NP, also displayed a notable increase in strength, specifically, a 50% increase in condition 1 and a 40% increase in condition 2. Mixture 1, the solely PC-binder mortar, displayed less change in strength, 15% and 25% for condition 1 and 2, respectively. While showing a lower total change in strength, the largest percent increase was exhibited by Mixture 4, the sodium carbonate activated AAM mortar; this mortar showed a 110% increase in strength between 7 days and 28 days in condition 2 and it showed a 205% increase in strength in condition 1. While the other AAM mortars did not exhibit as large of an increase in strength, they all showed increases greater than the PC mortar, between 25% and 45% depending on the AAM and curing condition.

Despite the considerable changes in compressive strength among the AAM mortars at longer curing periods, the highest strengths, regardless of testing age, were exhibited by the mortars containing PC. In curing condition 1, Mixture 2, the PC mixture with partial replacement of GBS, had the greatest 28-day strength, 31 MPa; in curing condition 2, Mixtures 1 and 2 displayed the highest 28-day strengths, ~26-27 MPa. Of the AAM mortars, the highest strength was shown by Mixture 5, which had 28-day strengths of 21 MPa and 19 MPa for curing

conditions 1 and 2, respectively. Mixture 5 was the only AAM mortar with strengths in the 20-30 MPa range that was exhibited by the mortars containing PC. A wide range of compressive strengths can be achieved in the production of AAMs (Habert *et al.,* 2011). The intent of this work was not to design AAM mortars to exceed compressive strength of PC mortars, which has been shown to be possible (Duran Atiş *et al.,* 2009), but rather to use controlled experimental assessments in conjunction with environmental impact assessments to gain a better understanding of how AAMs can be better engineered in the future. Differences in compressive strength as a function of curing condition were limited; few of the mixtures assessed showed a statistically significant difference between conditions. At each age, Mixture 7 showed a higher compressive strength when cured in condition 1; Mixture 5 also showed statistically significant increases at 7- and 28-day curing in condition 1 and Mixture 4 showed a significant increase in 14-day strength in condition 1. It is hypothesized that these variations may have been a function of improved leaching of alkali materials at the higher temperatures, which may have reduced reactive constituents slightly. However, as most specimens did not exhibit a significant change in strength between curing conditions, it is assumed that limited differences were likely a function of the low change in temperature and with a greater change in temperature, greater reactivity may have been noted.

Splitting Tensile Strength of Mortar

The 28-day splitting tensile strengths and 28-day compressive strengths for the mortars are presented in Table 3. Similar to the compressive strength data, the PC mortar specimens exhibited the highest tensile strengths ranging from 4-5 MPa. Again, of the AAMs, the highest strength was noted for Mixture 5: the split cylinder tensile strength for Mixture 5 was ~5 MPa for condition 1 and ~4 MPa for condition 2. Despite these consistencies in general trends, the

split cylinder tensile strength of the PC mortars was lower relative to their compressive strengths, ranging from 14-22% of the compressive strength, than for the AAM mortars, ranging from 21-33% of the compressive strength. This general increase in the ratio between tensile strength and compressive strength for AAMs was likely in part a reflection of the generally lower compressive strength previously noted for the AAMs and/or in part a reflection of the improved tensile properties noted for AAMs (Juenger *et al.*, 2011). For the AAM mortars, a wide range in compressive strengths was found: between 4 and 21 MPa. Similarly, a wide range in split tensile strength was noted: between 1 and 5 MPa. As with the compressive strength, most mixtures exhibited no statistically significant differences in tensile strength measurements for each mixture between the two curing conditions. The only exception was a slight increase in tensile strength for Mixture 7 in condition 1.

Mortar Moisture Absorption

The bulk densities, percent absorption, and percent void volume for each of the mortars are presented in Figure 6 normalized to Mixture 1, the solely PC powder mixture, in condition 1. The PC mortar specimens exhibited the highest bulk densities as well as the lowest percent absorptions and percent void volumes. The AAM mortars had bulk densities ranging from 89% to 97% those of the PC mortars, percent absorptions ranging from 130% to 170% of the PC mortars, and percent volume of voids ranging from 130% to 160% of the PC mortars. Of the AAM mortars, Mixture 5 had the highest bulk density, with the remaining AAMs exhibiting bulk densities within 5% of that of Mixture 5. It also had the lowest percent absorption and percent void volume, with the remaining AAM mortars exhibiting values within 20% of those of Mixture 5. Higher absorption and volume of voids could be indicative of potential durability issues; however, these values were recorded at a relatively early age and it is possible that with

459 continued gel evolution, these differences from the PC mortars may not have been as
460 pronounced.
461 As would be expected, the mortars exhibited correlations between bulk density, percent
462 absorption, percent void volume, and compressive strength. The linear correlation between
463 percent absorption and percent void volume was the strongest, $R^2 = 0.99$. The linear correlation
464 between percent absorption and bulk density as well as the correlation between void volume and
465 bulk density were lower, but still noteworthy, $R^2 = 0.92$ and 0.90, respectively. Trends continued
466 when each of these properties were compared to 28-day compressive strength of the mortars.
467 Bulk density showed the highest linear correlation to strength, $R^2 = 0.89$, but the linear
468 correlation between strength and absorption as well as that with void volume remained high, R^2
469 = 0.86 and 0.84, respectively. Such relationships can be expected as the porosity of cement-based
470 materials can be related to compressive strength and to each of the moisture-related properties
471 tested (Mehta and Monteiro 2006).
472 **Comparison and Discussion of LCA Results Normalized by Mechanical Properties**
473 Environmental impact comparisons of mixtures based on a constant volume of material
474 produced can be good indicators of environmental impacts that should be targeted for mitigation
475 strategies; however, because cementitious materials are often employed based upon certain
476 mechanical and durability traits, these properties should be incorporated into comparisons as
477 well. In this work, the compressive strength of the mortars at 7, 14, and 28 days were used in
478 conjunction with the GHG emissions quantified in the environmental impact assessments.
479 Compressive strength relative to the ratio of GHG emissions to compressive strength for each
480 mixture is plotted in Figure 7, showing how at different ages, the compressive strength changed
481 and as a result, the ratios changed. In these cases, a low ratio of environmental impact to

compressive strength would be desirable and would reflect either the ability to attain a higher strength or a lower environmental impact than the other mixtures analyzed.

As Figure 7 shows, on a per cubic meter basis, the AAMs displayed lower GHG emissions, as was discussed previously, but because the compressive strength achieved for these mixtures was lower than the PC mixtures, they did not consistently display a better environmental impact to strength ratio than the conventional mixtures. The relatively high strengths and low environmental impacts attained for the sodium sulfate activated AAMs, Mixture 5, led to this material achieving the best combination of environmental impact from production and strength at each age. The low GHG emissions from the sodium carbonate activated AAMs and their large strength development for the period of testing led to these mixtures offering the next lowest ratio at 28 days. However, based on their 7-day strength, several of the conventional mortar mixtures led to a better ratio of GHG emissions to compressive strength. Regardless of age, the sodium hydroxide mixture with elevated temperature curing resulted in the highest, and hence least desirable, ratio of GHG emissions to compressive strength. These results suggested that while lower GHG emissions could be achieved through replacement of cement with mineral admixtures or alternative binders, these changes should be made in context of the material properties desired. As was presented in this work, it is possible to have an AAM that consistently results in a better combination of compressive strength and GHG emissions relative to a PC-based mixture and it is possible to have an AAM that consistently results in a less desirable combination of properties.

The comparison method implemented to examine GHG emissions and compressive strength concurrently was also applied to tensile strength (see Figure 8). Because the AAM mortars possessed similar splitting strength to the PC-based mortars, while resulting in lower GHG

emissions from production, their ratios of GHG emissions to tensile strength were notably desirable. As with the ratios of GHG emissions to compressive strength, the lowest values for, and hence most desirable combination of low GHG emissions and high strength, were associated with Mixture 5. However, unlike the GHG emissions to compressive strength ratios, all but one AAM mortar, Mixture 7 cured using condition 2, resulted in lower ratios than the PC-based mortars. Namely, the AAM mortars resulted in 10 to 90% lower ratios of GHG emissions to split cylinder strength than the PC mortars, with the exception of Mixture 7 cured using condition 2, which offered an equivalent ratio to the PC mortars. These low ratios of emissions to tensile strength suggest the AAM mortars may be favorable in applications where tensile properties are critical.

It must be noted that the AAMs presented in this work scratch the surface of potential mixtures that can be produced through alkali-activation. Additionally, through alternative processing conditions (e.g., higher curing temperatures) it is possible that the mixtures assessed in this work would offer different mechanical properties. However, by providing an initial quantification of environmental impacts other than GHG emissions and by relating emissions to concrete properties, this work provides an initial step into understanding the potential benefits from utilizing AAMs over conventional PC mixtures.

Conclusions

In this research, mechanical property and environmental impact assessments were performed to examine alkali-activated materials (AAMs) for their potential to contribute to environmental impact mitigation in the cement-based materials industry. Assessments were performed for four AAM mortar mixtures containing 1:1 weight ratios of granulated blast-furnace slag (GBS) and natural pozzolans (NP) as the solid precursors. As a basis of comparison, assessments were also

performed on three mortars containing a typical hydraulic portland cement (PC) with and without partial replacement by ground GBS or NP. Some key findings from this work are:

- The AAM mortars batched for this work typically displayed lower compressive and tensile strength than the PC mortars; however, some AAM mortars were in a similar strength range and the literature shows large ranges in AAM mortar strength can be achieved.
- The AAM mortars, even with additional energy from higher temperature curing, consistently displayed lower greenhouse gas emissions, NO_X emissions, SO_X emissions, CO emissions, and Pb from production than the PC-based mortars.
- Despite the lower strengths of the AAM mortars than the PC mortars in this study, the significant reductions in greenhouse gas emissions from their production resulted in several AAM mortars exhibiting better greenhouse gas emissions to strength ratios than the PC mortars.

The assessments performed in this study focus on a small subset of AAM materials. The comparisons drawn using both mechanical properties and environmental impacts in this work suggest that AAMs may provide a desirable combination of traits to reduce environmental impacts relative to PC-based composites. However, more research is necessary in several areas to confirm their potential application as a means to mitigate environmental impacts. These include more robust assessment of durability of AAMs, such as susceptibility to deterioration under freeze/thaw conditions, ability to resist chloride ingress, and ability to withstand pH-induced deterioration. Further, future work should consider environmental impact assessments of other AAM mixtures as well as consider other environmental impacts beyond the emissions from production considered in this work.

The next stages of engineering AAMs should consider such durability and environmental impact parameters in their assessments to improve the environmental sustainability of these potential cementitious alternatives. Additionally, factors such as local resource availability, variation in material production methods, and costs associated with each stage of material acquisition through disposal should be evaluated. For example, in this work, a locally available pozzolan and an imported slag were utilized; in the future, these same resources may not be as prevalent or may be cost-prohibitive to use. Additionally, further study should be performed to ensure there are limited unintended consequences in environmental burdens from the use of AAMs.

Acknowledgements: The authors would like to thank Valerie Yanez and Kanotha Kamau-Devers at the University of California Davis for the assistance in the laboratory.

Data Availability Statement: Some or all data, models, or code generated or used during the study are available from the corresponding author by request (experimental data and life cycle impacts).

References

Abdalqader, A. F., F. Jin and A. Al-Tabbaa (2016). "Development of greener alkali-activated cement: utilisation of sodium carbonate for activating slag and fly ash mixtures." Journal of Cleaner Production **113**: 66-75.DOI: https://doi.org/10.1016/j.jclepro.2015.12.010.

ASTM (2013). ASTM C642-13: Standard Test Method for Density, Absorption, and Voids in Hardened Concrete. West Conshohoken, Pennsylvania, American Society for Testing Materials.

ASTM (2017a). ASTM C39/C39M - 17a: Standard Test Method for Compressive Strength of Cylindrical Concrete Specimens. West Conshohoken, Pennsylvania, American Society for Testing Materials.

ASTM (2017b). ASTM C496/C496M-17: Standard Test Method for Splitting Tensile Strength of Cylindrical Concrete Specimens. West Conshohoken, Pennsylvania, American Society for Testing Materials.

Bakharev, T. (2005). "Geopolymeric materials prepared using Class F fly ash and elevated temperature curing." Cement and Concrete Research **35**(6): 1224-1232.DOI: https://doi.org/10.1016/j.cemconres.2004.06.031.

CEC. (2018). "Total System Electric Generation." Retrieved May 24, 2018, from http://www.energy.ca.gov/almanac/electricity_data/total_system_power.html.

Celik, K., C. Meral, A. P. Gursel, P. K. Mehta, A. Horvath and P. J. M. Monteiro (2015). "Mechanical properties, durability, and life-cycle assessment of self-consolidating concrete mixtures made with blended portland cements containing fly ash and limestone powder." Cement and Concrete Composites **56**(0): 59-72.DOI: http://dx.doi.org/10.1016/j.cemconcomp.2014.11.003.

Chatterjee, A. K. (2011). "Chemistry and engineering of the clinkerization process — Incremental advances and lack of breakthroughs." Cement and Concrete Research **41**(7): 624-641.DOI: https://doi.org/10.1016/j.cemconres.2011.03.020.

Damineli, B. L., F. M. Kemeid, P. S. Aguiar and V. M. John (2010). "Measuring the eco-efficiency of cement use." Cement and Concrete Composites **32**(8): 555-562.DOI: http://dx.doi.org/10.1016/j.cemconcomp.2010.07.009.

Duran Atiş, C., C. Bilim, Ö. Çelik and O. Karahan (2009). "Influence of activator on the strength and drying shrinkage of alkali-activated slag mortar." Construction and Building Materials **23**(1): 548-555.DOI: https://doi.org/10.1016/j.conbuildmat.2007.10.011.

Gartner, E. and T. Sui (2018). "Alternative cement clinkers." Cement and Concrete Research **114**: 27-39.DOI: https://doi.org/10.1016/j.cemconres.2017.02.002.

Gomez, D. R., J. D. Watterson, B. B. Americano, C. Ha, G. Marland, E. Matsika, L. N. Namayanga, B. Osman-Elasha, J. D. K. Saka, K. Treanton and R. Quadrelli (2007). 2006 IPCC Guidelines for National Greenhouse Gas Inventories: Chapter 2: Energy: Stationary Combustion. S. Eggleston, L. Buendia, K. Miwa, T. Ngara and K. Tanabe. Hayama, Kanagawa, Intergovernmental Panel on Climate Change.

GREET (2010). The Greenhouse Gases, Regulated Emissions, and Energy Use In Transportation Model, GREET 1.8d.1. Argonne, IL.

Gursel, A. P. and A. Horvath. (2012). "GreenConcrete LCA Webtool." Retrieved November 13, 2014, from http://greenconcrete.berkeley.edu/concretewebtool.html.

Gursel, A. P., H. Maryman and C. Ostertag (2016). "A life-cycle approach to environmental, mechanical, and durability properties of "green" concrete mixes with rice husk ash." Journal of Cleaner Production **112, Part 1**: 823-836.DOI: http://dx.doi.org/10.1016/j.jclepro.2015.06.029.

Habert, G., J. B. d'Espinose de Lacaillerie and N. Roussel (2011). "An environmental evaluation of geopolymer based concrete production: reviewing current research trends." Journal of Cleaner Production **19**(11): 1229-1238.DOI: https://doi.org/10.1016/j.jclepro.2011.03.012.

Habert, G. and C. Ouellet-Plamondon (2016). "Recent update on the environmental impact of geopolymers." Rilem Technical Letters **1**: 17-23.DOI: https://doi.org/10.21809/rilemtechlett.2016.6.

Heath, A., K. Paine and M. McManus (2014). "Minimising the global warming potential of clas based geopolymers." Journal of Cleaner Production **78**: 75-83.DOI: https://doi.org/10.1016/j.jclepro.2014.04.046.

Jiang, M., X. Chen, F. Rajabipour and C. T. Hendrickson (2014). "Comparative Life Cycle Assessment of Conventional, Glass Powder, and Alkali-Activated Slag Concrete and Mortar." **20**(4): 04014020.DOI: doi:10.1061/(ASCE)IS.1943-555X.0000211.

Juenger, M. C. G., F. Winnefeld, J. L. Provis and J. H. Ideker (2011). "Advances in alternative cementitious binders." Cement and Concrete Research **41**(12): 1232-1243.DOI: https://doi.org/10.1016/j.cemconres.2010.11.012.

Kelly, T. D. and H. G. van Oss. (2014). "Historical Statistics for Mineral and Material Commodities: Cement Statistics." Retrieved January 1, 2015, from http://minerals.usgs.gov/minerals/pubs/historical-statistics/.

LTS. (2016). "DATASMART LCI Package (US-EI SimaPro® Library)." Retrieved October 4, 2018, from https://ltsexperts.com/services/software/datasmart-life-cycle-inventory/.
Marceau, M. L., M. A. Nisbet and M. G. VanGeem (2006). Life cycle inventory of Portland cement manufacture. Skokie, Illinois, Portland Cement Association.
Marceau, M. L., M. A. Nisbet and M. G. VanGeem (2007). Life Cycle Inventory of Portland Cement Concrete. Skokie, Illinois, Portland Cement Association.
McLellan, B. C., R. P. Williams, J. Lay, A. van Riessen and G. D. Corder (2011). "Costs and carbon emissions for geopolymer pastes in comparison to ordinary portland cement." Journal of Cleaner Production **19**(9–10): 1080-1090.DOI: http://dx.doi.org/10.1016/j.jclepro.2011.02.010.
Meddah, M. S. (2015). "Durability performance and engineering properties of shale and volcanic ashes concretes." Construction and Building Materials **79**: 73-82.
Mehta, P. K. and P. J. M. Monteiro (2006). Concrete : microstructure, properties, and materials. New York, McGraw-Hill.
Miller, S. A., P. R. Cunningham and J. T. Harvey (2019). "Rice-based ash in concrete: A review of past work and potential environmental sustainability." Resources, Conservation and Recycling **146**: 416-430.DOI: https://doi.org/10.1016/j.resconrec.2019.03.041.
Miller, S. A., A. Horvath and P. J. M. Monteiro (2016a). "Readily implementable techniques can cut annual CO2 emissions from the production of concrete by over 20%." Environmental Research Letters **11**: 074029.DOI: https://doi.org/10.1088/1748-9326/11/7/074029.
Miller, S. A., A. Horvath and P. J. M. Monteiro (2018a). "Impacts of booming concrete production on water resources worldwide." Nature Sustainability **1**(1): 69-76.DOI: https://doi.org/10.1038/s41893-017-0009-5.
Miller, S. A., V. M. John, S. A. Pacca and A. Horvath (2018b). "Carbon dioxide reduction potential in the global cement industry by 2050." Cement and Concrete Research **114**: 115-124.DOI: https://doi.org/10.1016/j.cemconres.2017.08.026.
Miller, S. A., P. J. M. Monteiro, C. P. Ostertag and A. Horvath (2016b). "Comparison indices for design and proportioning of concrete mixtures taking environmental impacts into account." Cement and Concrete Composites **68**: 131-143.DOI: http://dx.doi.org/10.1016/j.cemconcomp.2016.02.002.
Monteiro, P. J. M., S. A. Miller and A. Horvath (2017). "Towards sustainable concrete." Nature Materials **16**(7): 698-699.DOI: https://doi.org/10.1038/nmat4930
NREL. (2012). "U.S. Life Cycle Inventory Database." Retrieved November, 19, 2012, from https://www.lcacommons.gov/nrel/search.
Ohno, M. and V. C. Li (2018). "An integrated design method of Engineered Geopolymer Composite." Cement and Concrete Composites **88**: 73-85.DOI: https://doi.org/10.1016/j.cemconcomp.2018.02.001.
Oner, A. and S. Akyuz (2007). "An experimental study on optimum usage of GGBS for the compressive strength of concrete." Cement and Concrete Composites **29**(6): 505-514.DOI: http://dx.doi.org/10.1016/j.cemconcomp.2007.01.001.
Platts. (2014). "Steel Data and Analysis." Retrieved February 19, 2017, from http://www.platts.com/IM.Platts.Content/ProductsService/Products/steeldataanalysis.pdf.
Provis, J. L. (2018). "Alkali-activated binders." Cement and Concrete Research **114**: 40-48.DOI: https://dx.doi.org/10.1016/j.cemconres.2017.02.009.
Rattanasak, U. and P. Chindaprasirt (2009). "Influence of NaOH solution on the synthesis of fly ash geopolymer." Minerals Engineering **22**(12): 1073-1078.DOI: https://doi.org/10.1016/j.mineng.2009.03.022.

Robayo-Salazar, R., J. Mejía-Arcila, R. Mejía de Gutiérrez and E. Martínez (2018). "Life cycle assessment (LCA) of an alkali-activated binary concrete based on natural volcanic pozzolan: A comparative analysis to OPC concrete." Construction and Building Materials **176**: 103-111.DOI: https://doi.org/10.1016/j.conbuildmat.2018.05.017.
Ryu, G. S., Y. B. Lee, K. T. Koh and Y. S. Chung (2013). "The mechanical properties of fly ash-based geopolymer concrete with alkaline activators." Construction and Building Materials **47**: 409-418.DOI: https://doi.org/10.1016/j.conbuildmat.2013.05.069.
Sánchez Berriel, S., A. Favier, E. Rosa Domínguez, I. R. Sánchez Machado, U. Heierli, K. Scrivener, F. Martirena Hernández and G. Habert (2016). "Assessing the environmental and economic potential of Limestone Calcined Clay Cement in Cuba." Journal of Cleaner Production **124**: 361-369.DOI: https://doi.org/10.1016/j.jclepro.2016.02.125.
Scrivener, K., V. M. John and E. M. Gartner (2017). Eco-efficient cements: Potential economically viable solutions for a low-CO2 cement-based materials industry. Paris, France, United Nations Environment Programme
Solomon, S., D. Qin, M. Manning, Z. Chen, M. Marquis, K. B. Averyt, M. Tignor and H. L. Miller, Eds. (2007). Contribution of Working Group I to the Fourth Assessment Report of the Intergovernmental Panel on Climate Change. Cambridge, United Kingdom and New York, NY, USA, Cambridge University Press.
Teh, S. H., T. Wiedmann, A. Castel and J. de Burgh (2017). "Hybrid life cycle assessment of greenhouse gas emissions from cement, concrete and geopolymer concrete in Australia." Journal of Cleaner Production **152**(Supplement C): 312-320.DOI: https://doi.org/10.1016/j.jclepro.2017.03.122.
Turner, L. K. and F. G. Collins (2013). "Carbon dioxide equivalent (CO2-e) emissions: A comparison between geopolymer and OPC cement concrete." Construction and Building Materials **43**: 125-130.DOI: https://doi.org/10.1016/j.conbuildmat.2013.01.023.
USDOE (2015). State of Pennsylvania Energy Sector Risk Profile, Office of Electricity Delivery and Energy Reliability, United States Department of Energy.
USDOE (2016). State of Nevada Energy Sector Risk Profile, Office of Electricity Delivery and Energy Reliability, United States Department of Energy.
USEPA (1995a). AP 42, Fifth Edition, Volume I Chapter 1: External Combustion Sources. Research Triangle Park, NC.
USEPA (1995b). AP 42, Fifth Edition, Volume I Chapter 11: Minerals Products Industry. Research Triangle Park, NC.
USEPA (2001). Air Emissions Inventories, Volume 2 Chapter 14: Uncontrolled Emission Factor Listing for Criteria Air Pollutants.
van Oss, H. G. (2015). Minerals yearbook: cement 2012, United States Geological Survey**:** 16.11-16.38. .
van Oss, H. G. (2017). Mineral Commodity Summaries: Cement. , US Geological Survey.
Yang, K.-H., K.-H. Lee, J.-K. Song and M.-H. Gong (2014). "Properties and sustainability of alkali-activated slag foamed concrete." Journal of Cleaner Production **68**: 226-233.DOI: https://doi.org/10.1016/j.jclepro.2013.12.068.
Yang, K.-H., J.-K. Song and K.-I. Song (2013). "Assessment of CO2 reduction of alkali-activated concrete." Journal of Cleaner Production **39**: 265-272.DOI: https://doi.org/10.1016/j.jclepro.2012.08.001.

Zhuang, X. Y., L. Chen, S. Komarneni, C. H. Zhou, D. S. Tong, H. M. Yang, W. H. Yu and H. Wang (2016). "Fly ash-based geopolymer: clean production, properties and applications." Journal of Cleaner Production **125**: 253-267.DOI: https://doi.org/10.1016/j.jclepro.2016.03.019.

Figures and captions

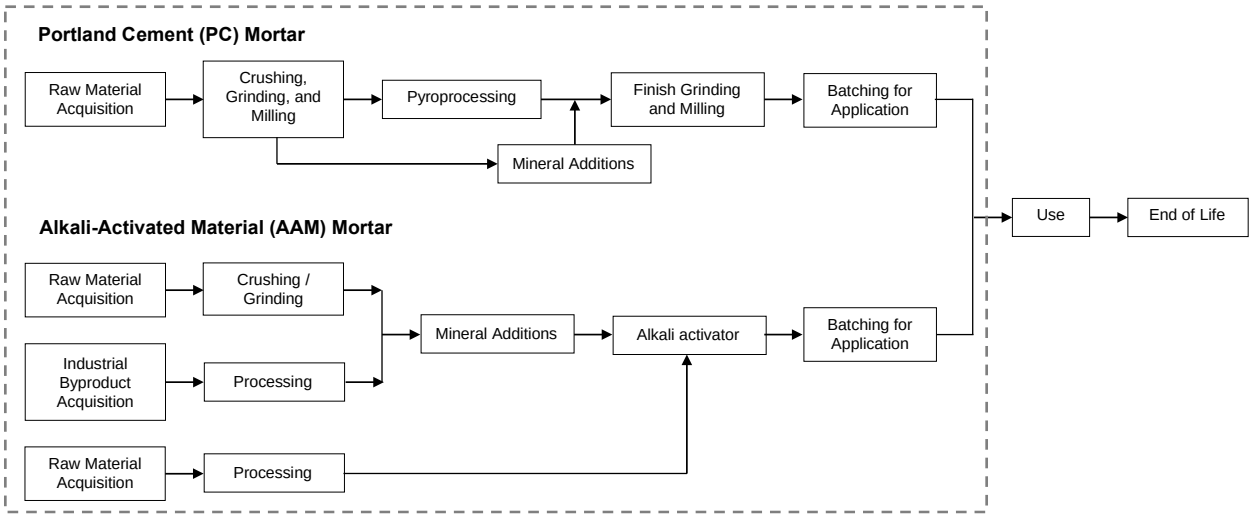

Fig. 1. Process flow diagram for the production of portland cement binder mortar and alkali-activated material mortar. Dashed line indicates processes considered in the life cycle inventory.

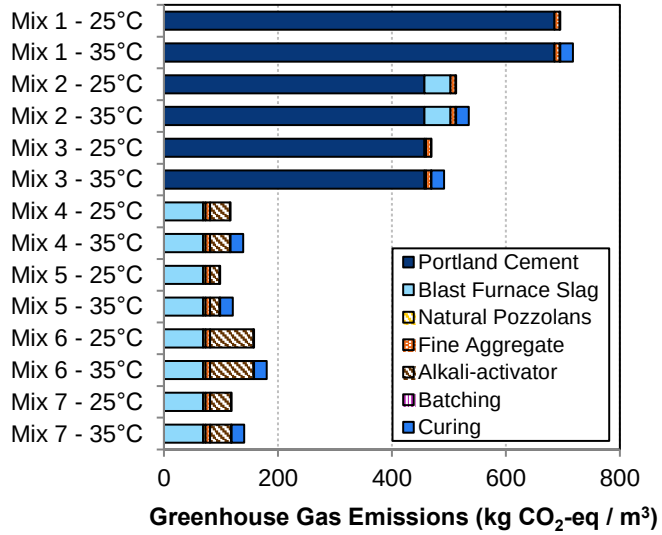

Fig. 2. Greenhouse gas emissions per cubic meter of mortar

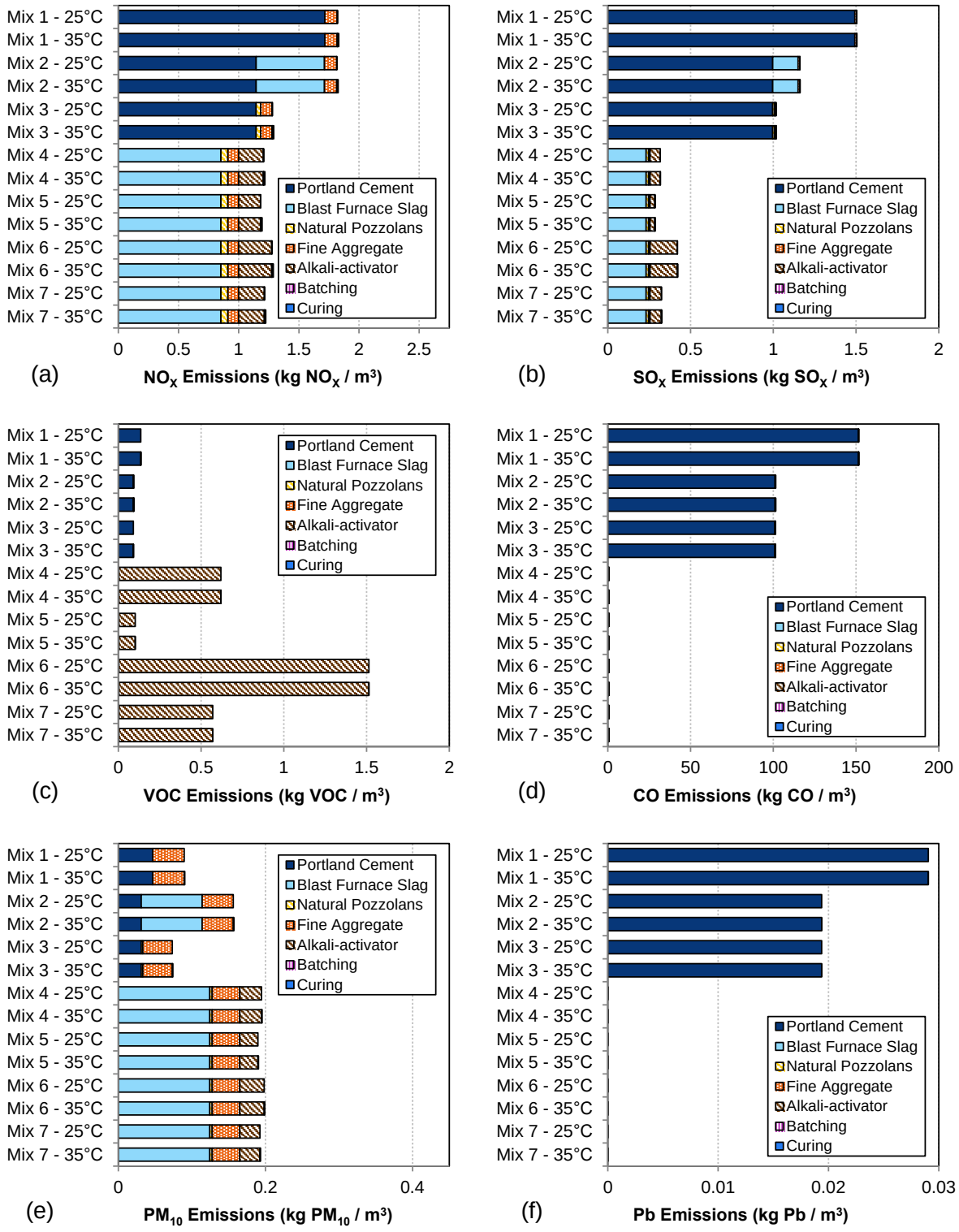

732

733 **Fig. 3.** Air pollutant emissions per cubic meter of mortar, namely: (a) NO_X emissions; (b) SO_X

734 emissions; (c) VOC emissions; (d) CO emissions; (e) PM_{10} emissions; and (f) Pb emissions

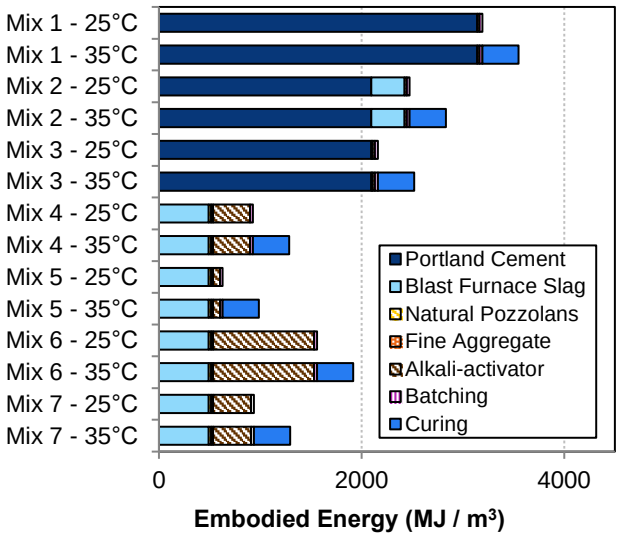

735

736 **Fig. 4.** Embodied energy per cubic meter of mortar

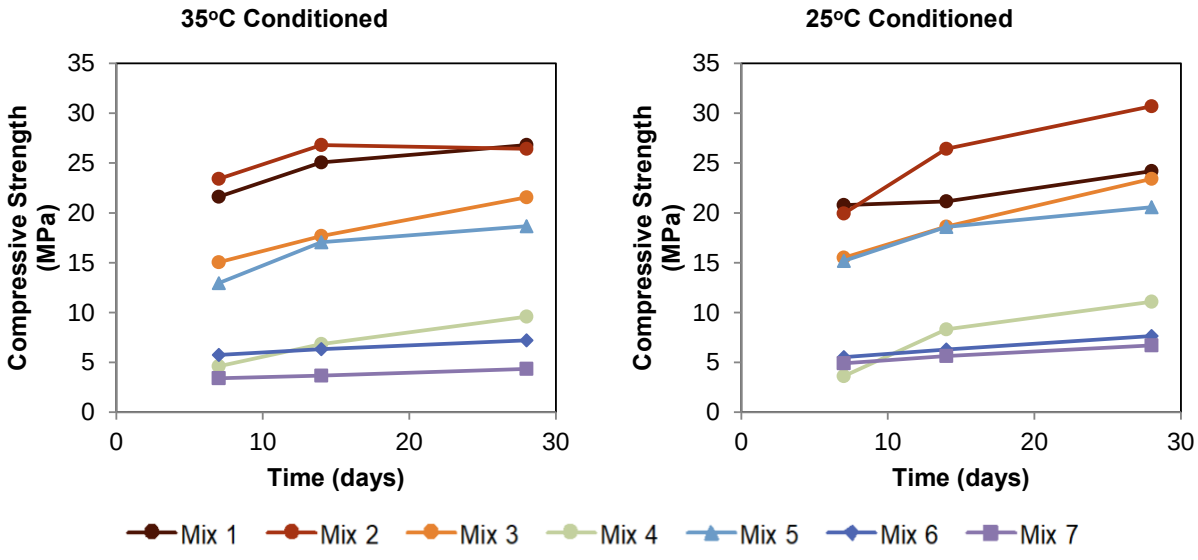

737

738 **Fig. 5.** Compressive strength development at 7-, 14-, and 28-day testing intervals.

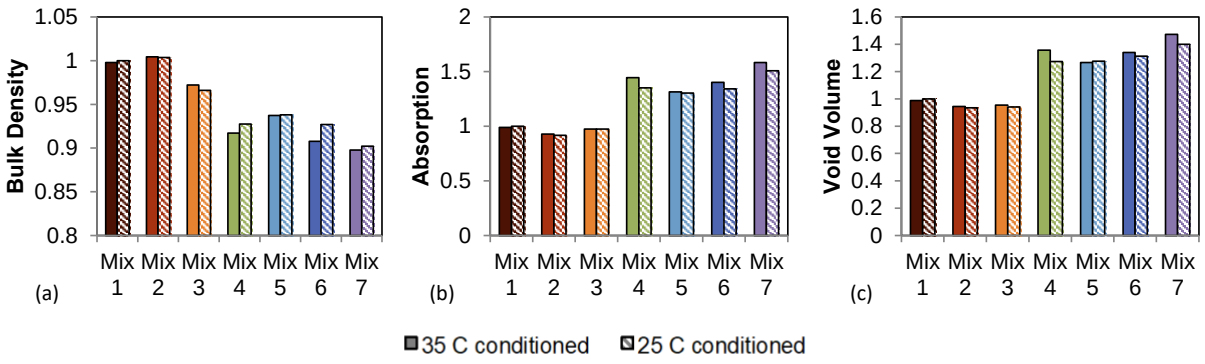

739

740 **Fig. 6.** (a) Bulk density, (b) absorption, and (c) void volume for each mortar mixture under each

741 of two curing conditions. Values are normalized to Mixture 1 cured in ambient temperature.

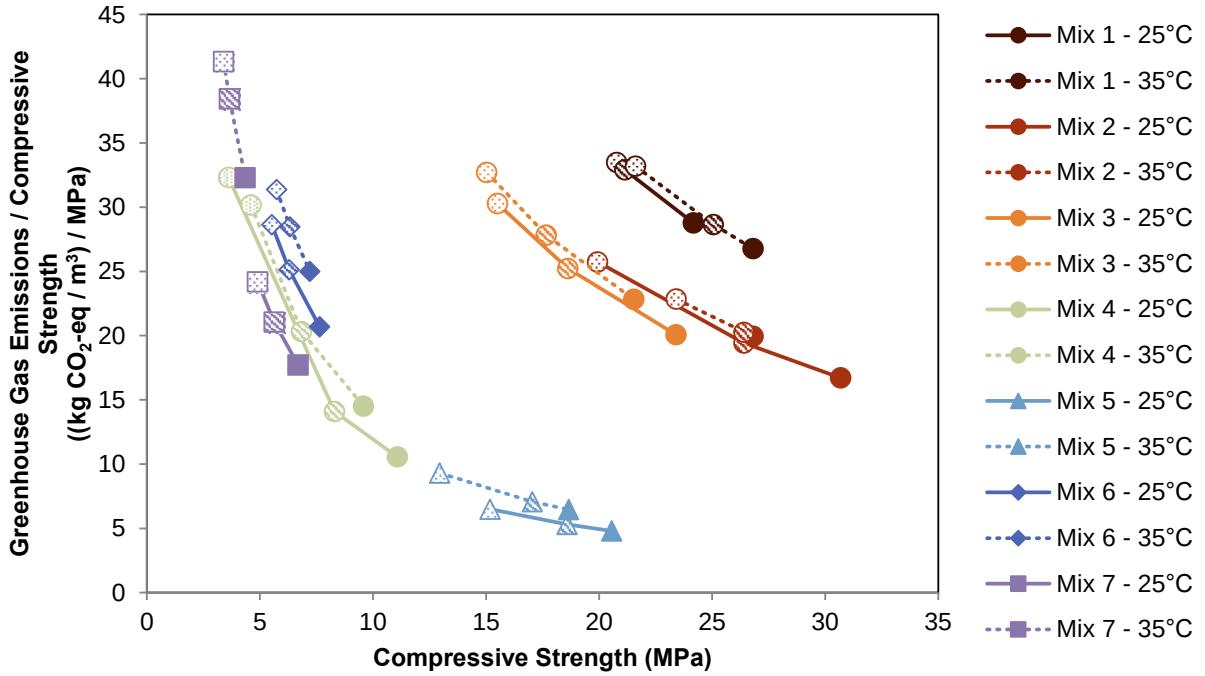

742

743 **Fig. 7.** Compressive strength plotted against the ratio of greenhouse gas emissions per cubic

744 meter of mortar per MPa of compressive strength. (⚪) indicates the ratio taken for strength at 7

745 days; (▨) indicates the ratio taken for strength at 14 days; (●)indicates the ratio taken for

746 strength at 28 days.

747

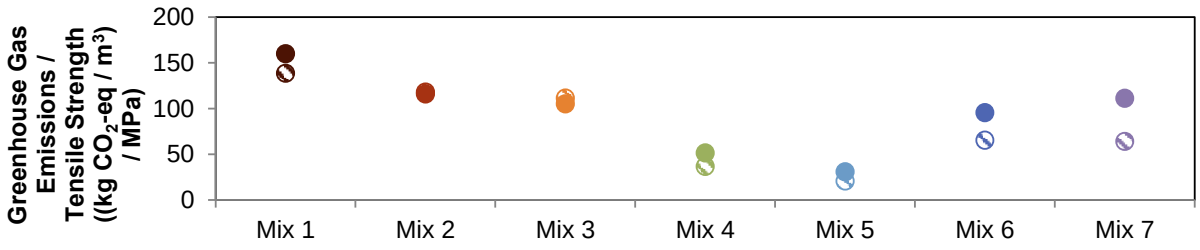

748

749 **Fig. 8.** The ratio of greenhouse gas emissions per cubic meter of mortar to spilt cylinder tensile

750 strength. (▨) indicates mixtures cured at 25°C; (●) indicates mixtures cured at 35°C.

751 **Table 1.** Mixture proportions for mortar examined

Mixtures	water (kg/m^3)	cement (kg/m^3)	GBS (kg/m^3)	NP (kg/m^3)	Sand (kg/m^3)	NaOH (kg/m^3)	Na_2CO_3 (kg/m^3)	Na_2SO_4 (kg/m^3)
1	350	700	0	0	1131.7	0	0	0
2	350	466.9	233.1	0	1116.9	0	0	0
3	350	466.9	0	233.1	1053.9	0	0	0
4	350	0	350	350	992.6	0	18.75	0
5	350	0	350	350	992.6	0	0	6.94
6	350	0	350	350	992.6	50	0	0
7	350	0	350	350	992.6	18.75	0	0

752
753

754 **Table 2.** Cement processing assumptions to calculate electricity requirements

Process	Technology
Cement prehomogenization	Dry process, raw storing, non-blending
Cement raw materials grinding	Dry, raw grinding, ball mill
Cement raw meal blending	Dry, raw meal homogenization, blending, and storage
Clinker cooling	Reciprocating grate cooler
Cement finish milling	Ball mill
Conveying within the cement plant	Screw pump, conveyed 20m

755
756

Table 3. Mortar 28-day compressive strength and 28-day tensile strength by mixture proportion and curing condition (terms in parenthesis denote standard deviation)

Mixtures	Curing Condition (1 or 2)	Compressive Strength (MPa)		Tensile Strength (MPa)	
1	1	24.18	(1.93)	5.01	(0.18)
	2	26.81	(3.46)	4.48	(1.41)
2	1	30.69	(1.39)	4.33	(1.02)
	2	26.41	(3.24)	4.61	(1.33)
3	1	23.41	(0.98)	4.21	(0.56)
	2	21.54	(0.98)	4.66	(0.54)
4	1	11.08	(0.87)	3.16	(0.61)
	2	9.58	(0.49)	2.69	(0.25)
5	1	20.56	(0.79)	4.74	(0.35)
	2	18.65	(0.29)	3.90	(0.95)
6	1	7.64	(0.23)	2.41	(0.33)
	2	7.21	(0.28)	1.88	(0.45)
7	1	6.69	(0.11)	1.85	(0.22)
	2	4.35	(0.17)	1.26	(0.24)